Laser-modified electron correlations and deflection of atoms by laser light

O. Zobay and G. Alber
Theoretische Quantendynamik, Fakultät für Physik, Universität Freiburg, D-79104 Freiburg im Breisgau, Germany
(Received 16 August 1996)

The influence of laser-induced two-electron excitation processes on the deflection of atoms by a standing-wave laser field is investigated. In particular, isolated-core excitation processes are studied in which, after preparing one valence electron as an electronic Rydberg wave packet, the core electron is driven resonantly by the standing wave. The dynamics of the two electrons are entangled through laser-induced electron correlation effects. A theoretical approach is developed that clearly exhibits the intricate interplay between these correlation effects and the atomic center-of-mass motion that originates from the stimulated light force. Various examples are analyzed that show the manifestations of this interplay in the diffraction pattern of a deflected atom. [S1050-2947(97)06610-9]

PACS number(s): 42.50.Vk, 03.75.Be, 32.80.−t

I. INTRODUCTION

Recent advances in the field of atom optics have renewed interest in the deflection of atoms by stimulated light forces and the basic physical mechanisms that are responsible for it [1–5]. The momentum transfer from a laser field to the atomic center of mass is characterized by the fact that it proceeds essentially only by excitation of the internal electronic degrees of freedom of the atom. This is due to the large mass difference between the atomic nucleus and electrons. The resulting strong laser-induced correlation between the internal electronic dynamics of an atom and its center-of-mass motion offers the possibilities (i) to deflect atoms in a controlled way by an appropriate choice of the laser-induced electronic excitation process and (ii) to investigate the internal laser-modified electronic dynamics of an atom by observation of its center-of-mass motion. It has been shown that for these purposes the high-level density of Rydberg systems offers interesting perspectives [6–8]. In these studies schemes for atomic beam deflection were investigated in which the coherent momentum transfer from a standing-wave laser field to the atom depends strongly on whether the laser field excites an isolated or a large number of Rydberg states. In the former case the momentum exchange is dominated by the wave aspects of the electronic dynamics, in the latter case by particle aspects of the Rydberg electron. So far most studies on laser-induced correlations between atomic center-of-mass motion and the internal electronic dynamics have concentrated on laser excitation processes that involve a single valence electron only.

In view of these developments the natural question arises how laser-induced two-electron excitation processes and the resulting electron correlation effects influence the stimulated light force. It is the main aim of this paper to explore this question theoretically and to investigate the coherent momentum exchange between a standing-wave laser field and the atomic center of mass that results from such excitation processes. A basic two-electron excitation process that has received considerable attention recently from both experimental and theoretical points of view is isolated core excitation (ICE) [9,10]. Thereby two valence electrons, typically of an alkaline-earth atom, are excited optically in a two-step process. In the first step one of these valence electrons is excited to a Rydberg state close to the photoionization threshold. Subsequently, the other electron is excited to one of the lowest excited states of the ionic core. The electrons influence each other by electron correlation effects. Recent work on laser-induced ICE processes has concentrated predominantly on the question of how Rabi oscillations of a resonantly excited ionic core influence the dynamics of the Rydberg electron via these electron correlation effects. Both time-independent [11] and time-dependent [12–16] studies have been performed and have demonstrated, for example, that the resulting laser-modified electron correlations of a resonantly excited core may even cause a suppression of autoionization [14]. However, vice versa, the dynamics of the excited Rydberg electron also influences the laser-induced transitions of the core electron. This influence of the excited Rydberg electron on the dynamics of the core electron manifests itself, for example, in the characteristics of the spontaneous emission of photons by the ionic core [17]. Furthermore, the dynamics of the Rydberg electron also influences the processes by which momentum is transferred from a standing-wave laser field, which drives the core electron resonantly, to the atomic center of mass. In the following this latter aspect will be investigated in detail by considering the deflection of fast atoms by a standing-wave laser field. In this case the Raman-Nath approximation [2] can be employed and the intricate relation between the atomic center-of-mass motion and the internal, laser-modified dynamics of the electrons can be worked out most clearly. Our theoretical approach will be based on semiclassical path representations of the relevant transition amplitudes. Thereby these amplitudes are expanded into a sum of contributions that are associated with repeated returns of the excited Rydberg electron to the ionic core. The scattering processes induced by electron correlation effects and the laser-induced excitation processes, which both take place inside the core region, may easily be taken into account with the help of quantum defect theory [15,18].

This paper is organized as follows. In Sec. II the deflection of fast atoms by a standing-wave laser field is discussed within the framework of an effective two-channel problem. This model problem is capable of describing the basic physi-

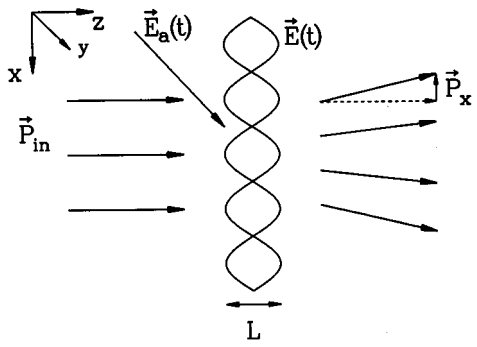

FIG. 1. Setup for the model problem of Sec. II A: After the atom has entered the standing-wave field $\mathbf{E}(t)$, the short pulse $\mathbf{E}_a(t)$ is applied. By preparing the Rydberg wave packet, the pulse triggers the Rabi oscillations of the core and thereby the momentum transfer to the atomic center of mass.

cal processes that result from the simultaneous excitation of two valence electrons during the flight of an atom through a standing-wave laser field. For the transition amplitudes that describe the deflection of atoms by this laser field a semiclassical path representation is developed with respect to the orbital round-trips of the excited Rydberg valence electron around the nucleus. This theoretical approach exhibits clearly the intricate interplay between laser-modified electron correlation effects and the atomic center-of-mass motion during the interaction of an atom with a standing-wave laser field. The physical contents of these theoretical developments and numerical examples are discussed in Sec. III. Conclusions are given in Sec. IV.

II. THEORETICAL DESCRIPTION OF ATOMIC DEFLECTION BY LASER-INDUCED CORE EXCITATION

A. Model problem

In order to present the main ideas most clearly, in this section an idealized model problem is examined, which is depicted in Fig. 1. Aspects of possible experimental realizations will be discussed in Sec. II B. In the following, Hartree atomic units are used.

An atom, e.g., an alkaline-earth atom, with mass M and well-defined initial momentum $\mathbf{P}_{\rm in}$ of its center of mass traverses a standing-wave laser field at right angles. The electric-field strength at the position of the atomic center of mass $\mathbf{R}$ is given by

$$\mathbf{E}(\mathbf{R},t)=\mathcal{E}(\mathbf{R})\mathbf{e}e^{-i\omega t}+\text{c.c.}, \tag{1}$$

with ω and $\mathbf{e}$ denoting field frequency and polarization. The standing-wave envelope is approximated by

$$\mathcal{E}(\mathbf{R})=\Theta(z)\Theta(L-z)\mathcal{E}(x), \tag{2}$$

with

$$\mathcal{E}(x)=\mathcal{E}_0\ \sin(kx). \tag{3}$$

The modulus of the wave vector is denoted by k. Initially, at $t=0$ immediately before entering the standing-wave laser field, the atom is prepared in an energetically low-lying bound electronic state $|g\rangle$ with energy ε_g. The standing-wave laser field is assumed to be tuned in resonance with a transition of the ionic core from its ground state (energy ε_1) to an excited state (energy ε_2). Due to electron correlation effects, in general, the standing-wave laser field will be well detuned from any excitation of the atomic state $|g\rangle$. Thus the atom will not be excited significantly by the standing-wave laser field so that the light force exerted on it may be neglected. After entering the standing-wave field $\mathbf{E}(\mathbf{R},t)$ the atom is exposed to a short (running wave) laser pulse

$$\mathbf{E}_a(t)=\mathcal{E}_a(t)\mathbf{e}_a e^{i(k_a y-\omega_a t)}+\text{c.c.}, \tag{4}$$

with polarization $\mathbf{e}_a$ and frequency ω_a, which propagates with wave vector $k_a\mathbf{e}_y$ along the y direction perpendicular to the incoming atom and the standing-wave field. This choice of direction of propagation implies that the short pulse transfers at most only one unit of photon momentum $k_a\mathbf{e}_y$ to the atom. The pulse envelope is assumed to be centered around time t_0 and is taken to be of the form

$$\mathcal{E}_a(t)=\mathcal{E}_a^{(0)}\ \exp[-4(\ln 2)(t-t_0)^2/\tau^2]. \tag{5}$$

It is also assumed that the pulse duration τ is short in comparison to the time of flight of the atom through the standing-wave laser field. The frequency ω_a is chosen such that the atom is excited from $|g\rangle$ to high-lying Rydberg states close to the first photoionization threshold. If the pulse duration τ is short in comparison to the classical orbit time of the excited Rydberg states, a radial Rydberg wave packet is created that orbits around the nucleus. In addition, however, the standing-wave laser field $\mathbf{E}(\mathbf{R},t)$ will excite the ionic core resonantly as soon as the electronic wave packet is prepared. The subsequent Rabi oscillations of the ionic core will transfer momentum from the standing-wave laser field to the atomic center of mass coherently by the stimulated light force. Contrary to the well-known case of a resonantly coupled two-level system, this momentum transfer will be influenced by the dynamics of the excited electronic Rydberg wave packet via electron correlation effects, namely, shakeup and autoionization. Thus, when leaving the standing-wave laser field the momentum distribution of the atom's center of mass will contain information about the dynamics of the Rydberg electron and the electron correlation effects during the interaction with the laser field.

In general, three main contributions can be distinguished in the momentum distribution. (i) If the atom has not been excited by the short laser pulse it will leave the standing-wave laser field undeflected, approximately. Alternatively, in case a Rydberg wave packet has been prepared by the short laser pulse the atom may leave the standing-wave laser field with its core either in the ground or in the excited state. (ii) If the core is excited, the atom will autoionize and the resulting ion can be removed easily by a static electric field. (iii) If after the interaction with the standing-wave laser field the core is in its ground state, the atom will not autoionize and thus will remain neutral. Therefore, a natural observable that contains information about the influence of the Rydberg electron on the core electron during the interaction with the standing-wave laser field is the momentum distribution of atoms that leave the interaction region with their core in the ground state. To obtain further insights, the measurement of this momentum distribution may be also performed state se-

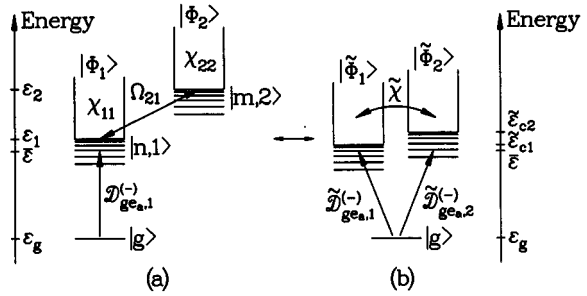

FIG. 2. Excitation scheme describing the internal atomic dynamics: (a) bare Rydberg series and (b) ''dressed'' Rydberg series.

lectively with respect to the excited Rydberg electron by means of ramped field ionization [10].

The interplay between laser-modified electron correlation effects and the atomic center-of-mass motion is exhibited in a particularly transparent way in the case of fast atoms. Atoms are considered to be fast if their kinetic energy is much larger than the electronic interaction energy with the exciting laser fields and if their deflection inside the laser field is small in comparison to the wavelength of the standing wave. These conditions imply that inside the laser field the atomic center of mass moves with constant velocity $v_{\rm in}=|\mathbf{P}|_{\rm in}/M$ on a straight-line trajectory perpendicular to the standing-wave laser field. Under these conditions the eikonal [19] and Raman-Nath [2] approximations can be used in the theoretical description. Thus the state $\langle x|\psi(\mathcal{T})\rangle$ of an atom, which has crossed the standing-wave laser field at position x with an effective interaction time of $\mathcal{T}=L/v_{\rm in}-t_0$, can be decomposed into the components of the almost resonantly coupled electronic states. For the two-channel excitation scheme depicted in Fig. 2 it is found that

$$\langle x|\psi(\mathcal{T})\rangle = a_g^{(\mathcal{T})}(x)|g\rangle + \sum_n a_{n,1}^{(\mathcal{T})}(x)|n,1\rangle|\Phi_1\rangle + \sum_m a_{m,2}^{(\mathcal{T})}(x)|m,2\rangle|\Phi_2\rangle. \tag{6}$$

The summations in Eq. (6) refer to both Rydberg and continuum states. The probability amplitude in the initial state $|g\rangle$, i.e., $a_g^{(\mathcal{T})}(x)$, and the excited Rydberg states in channels 1 and 2, i.e., $a_{n,1}^{(\mathcal{T})}(x)$ and $a_{m,2}^{(\mathcal{T})}(x)$, are determined by solving the time-dependent Schrödinger equation with the Hamiltonian

$$H(x)=H_{\rm atom}+V_{\rm ICE}(x)+V_{\rm pump}(t). \tag{7}$$

In the two-channel approximation the atomic Hamiltonian is given by

$$H_{\rm atom}=\varepsilon_g|g\rangle\langle g|+\sum_{j=1,2}[\mathbf{h}_{jj}+\mathbf{V}_{jj}(r)+\varepsilon_{cj}]|\Phi_j\rangle\langle\Phi_j|. \tag{8}$$

The channel states $|\Phi_1\rangle$ and $|\Phi_2\rangle$ represent the ground state and excited state of the ionic core [18,20]. The atomic eigenstates in channel j are denoted $|n,j\rangle|\Phi_j\rangle$. The radial Hamiltonian of the Rydberg electron in channel j with angular momentum l_j is given by $\mathbf{h}_{jj}+\mathbf{V}_{jj}(r)+\epsilon_{cj}$, with

$$\mathbf{h}_{jj}=-\frac{1}{2}\frac{d^2}{dr^2}+\frac{l_j(l_j+1)}{2r^2}-\frac{1}{r}.$$

The short-range potential $\mathbf{V}_{jj}(r)$ describes the effects of the residual core electrons. The radial coordinate of the Rydberg electron is denoted by r. As the excited channels have opposite parities there is no configuration interaction potential $V_{12}(r)$ coupling the two channels. In an ICE transition the angular momentum of the Rydberg electron is conserved so that $l_1=l_2=l$ [10]. In the rotating-wave approximation the channel thresholds are given by $\varepsilon_{c1}=\varepsilon_1$, $\varepsilon_{c2}=\varepsilon_2-\omega$. According to standard treatments of ICE processes [10,12,21] in the dipole and rotating-wave approximation the coupling of channels 1 and 2 induced by the standing-wave field can be modeled as

$$V_{\rm ICE}(x)=-\frac{1}{2}\Omega_{21}(x)(|\Phi_1\rangle\langle\Phi_2|+|\Phi_2\rangle\langle\Phi_1|). \tag{9}$$

Thereby, the position-dependent, real-valued Rabi frequency of the core transition is denoted

$$\Omega_{21}(x)=2\langle\Phi_2|\mathbf{d}\cdot\mathbf{e}|\Phi_1\rangle\mathcal{E}(x), \tag{10}$$

with the atomic dipole operator $\mathbf{d}$. The interaction of the atom with the short laser pulse is described by

$$V_{\rm pump}(t)=-\mathbf{d}\cdot\mathbf{e}_a\mathcal{E}_a(t)e^{-i\omega_a t}+\text{H.c.} \tag{11}$$

The main purpose of the applied pump pulse $\mathcal{E}_a(t)$ is to prepare an electronic Rydberg wave packet and to trigger the Rabi oscillations of the ionic core. Thus, for the sake of simplicity, it will be assumed in the following that this pump field is sufficiently weak so that its influence on the atomic dynamics can be described perturbatively. In this case it is found [22] that

$$a_{n,1}^{(\mathcal{T})}(x)=ie^{-i\overline{\varepsilon}t_0}\langle n,1|\langle\Phi_1|e^{-iH_0(x)\mathcal{T}}\tilde{\mathcal{E}}_a(H_0(x)-\overline{\varepsilon})\mathbf{d}\cdot\mathbf{e}_a|g\rangle, \tag{12}$$

with the mean excited energy $\overline{\varepsilon}=\varepsilon_g+\omega_a$. The Fourier transform of the pump field envelope is given by

$$\tilde{\mathcal{E}}_a(\varepsilon)=\int_{-\infty}^{\infty}dt'\,\mathcal{E}_a(t')e^{i\varepsilon(t'-t_0)} \tag{13}$$

and $H_0(x)=H_{\rm atom}+V_{\rm ICE}(x)$.

The probability amplitude of observing after its flight through the standing-wave field a deflected atom in state $|n,1\rangle|\Phi_1\rangle$ with transverse momentum p_x is given by [2]

$$a_{n,1}^{(\mathcal{T})}(p_x)=\frac{1}{\lambda}\int_0^{\lambda}dx\;a_{n,1}^{(\mathcal{T})}(x)e^{-ip_x x}, \tag{14}$$

with $\lambda=2\pi/k$ the wavelength of the standing wave. Equation (14) shows how the state-selective atomic transition amplitude $a_{n,1}^{(\mathcal{T})}(x)$ acts as a diffraction grating for the atomic center-of-mass motion. This diffraction grating is determined by the interaction of the two valence electrons with the laser fields. In order to exhibit clearly the influence of the electronic Rydberg wave packet on the atomic diffraction pro-

cess it is convenient to use a semiclassical path representation for $a_{n,1}^{(\mathcal{T})}(x)$. As outlined in the Appendix, this representation is given by

$$a_{n,1}^{(\mathcal{T})}(x)=e^{-i\overline{\varepsilon}t_0}\frac{(-1)^l}{2\pi i}\sum_{M=0}^{\infty}\int_{-\infty+i0}^{\infty+i0} \times d\varepsilon e^{-i\varepsilon\mathcal{T}}\nu_n^{-3/2}[e^{i\pi\nu_n}\mathbf{w}(x)-e^{-i\pi\nu_n}\mathbf{w}(x)e^{2\pi i\tilde{\boldsymbol{\nu}}(x)}] \times[\tilde{\boldsymbol{\chi}}(x)e^{2\pi i\tilde{\boldsymbol{\nu}}(x)}]^M\tilde{\boldsymbol{\mathcal{D}}}_{g\mathbf{e}_a}^{(-)}(x)\tilde{\mathcal{E}}_a(\varepsilon-\overline{\varepsilon}). \quad (15)$$

This is a main result of this section. It shows explicitly how the repeated returns of the excited Rydberg electron to the ionic core influence the spatial dependence of the probability amplitudes $a_{n,1}^{(\mathcal{T})}(x)$. According to Eq. (14), this spatial dependence determines the momentum distribution of the deflected atoms.

In Eq. (15) all quantities with a tilde refer to components in the basis of photon-dressed core states $|\tilde{\Phi}_i(x)\rangle$ [11,15]. In the case of a real-valued Rabi frequency $\Omega_{21}(x)$ these photon-dressed core states are related to the bare core states $|\Phi_j\rangle$ by an orthogonal transformation $\mathbf{O}(x)$, i.e., $|\tilde{\Phi}_i(x)\rangle=\Sigma_{j=1,2}\mathbf{O}_{ij}^T(x)|\Phi_j\rangle$. The orthogonal transformation $\mathbf{O}(x)$ diagonalizes the laser-induced coupling of the ionic core, i.e.,

$$\mathbf{O}^T(x)\begin{pmatrix}\varepsilon_{c1} & -\frac{1}{2}\Omega_{21}(x)\\ -\frac{1}{2}\Omega_{21}(x) & \varepsilon_{c2}\end{pmatrix}\mathbf{O}(x)=\tilde{\boldsymbol{\varepsilon}}_c(x). \quad (16)$$

The diagonal matrix $\tilde{\boldsymbol{\varepsilon}}_c(x)$ contains the position-dependent energies of the dressed states of the ionic core. The matrix elements of the 2×2 diagonal matrix $\tilde{\boldsymbol{\nu}}(x)$ are given by $\tilde{\boldsymbol{\nu}}_{jj}(x)=\{2[\tilde{\varepsilon}_{cj}(x)-\varepsilon]\}^{-1/2}$. The scattering matrix $\tilde{\boldsymbol{\chi}}(x)$ describes scattering of the excited Rydberg electron between the photon-dressed core channels. This scattering takes place inside the core region. The matrix $\tilde{\boldsymbol{\chi}}(x)$ is related to the diagonal bare scattering matrix $\boldsymbol{\chi}$ by

$$\tilde{\boldsymbol{\chi}}(x)=\mathbf{O}^T(x)\boldsymbol{\chi}\mathbf{O}(x). \quad (17)$$

The matrix elements of the diagonal bare scattering matrix are given by $\boldsymbol{\chi}_{jj}=e^{2\pi i\mu_j}$, with μ_j denoting the quantum defects of the bare channels. The (energy-normalized) photoionization dipole matrix elements [18,20] that characterize the laser-induced excitation of the dressed channels by the weak pump field $\mathcal{E}_a(t)$ are denoted by the column vector $\tilde{\boldsymbol{\mathcal{D}}}_{g\mathbf{e}_a}^{(-)}(x)=\mathbf{O}^T(x)\boldsymbol{\mathcal{D}}_{g\mathbf{e}_a}^{(-)}$. In the excitation scheme of Fig. 2 it is assumed that the initial state $|g\rangle$ excites Rydberg states in channel 1 only. This means that the component $(\boldsymbol{\mathcal{D}}_{g\mathbf{e}_a}^{(-)})_2$ vanishes and that $(\boldsymbol{\mathcal{D}}_{g\mathbf{e}_a}^{(-)})_1=-ie^{i\pi\mu_1}d_{\varepsilon g}$ with $d_{\varepsilon g}$ the standing-wave dipole matrix element between state $|g\rangle$ and the continuum states of channel 1. The row vector $\mathbf{w}(x)$ has components $\mathbf{w}_i(x)=\mathbf{O}_{1i}(x)/[\varepsilon_{n,1}-\varepsilon_{c1}-\varepsilon+\tilde{\varepsilon}_{cj}(x)]$. By inserting Eq. (15) into Eq. (14) one arrives at the semiclassical path representation for the transverse momentum distribution. In Eq. (15) the quantities $\mathbf{w}(x)$, $\tilde{\boldsymbol{\chi}}(x)$, $\tilde{\boldsymbol{\nu}}(x)$, and $\tilde{\boldsymbol{\mathcal{D}}}_{g\mathbf{e}_a}^{(-)}(x)$ depend on the position x at which an atom crosses the standing-wave laser field. If, however, the standing-wave field is tuned in resonance with the core transition, i.e., $\Delta=\varepsilon_{c2}-\varepsilon_{c1}=0$, $\tilde{\boldsymbol{\chi}}(x)$ and $\tilde{\boldsymbol{\mathcal{D}}}_{g\mathbf{e}_a}^{(-)}(x)$ become independent of x. The effective quantum number of the Rydberg state $|n,1\rangle|\Phi_1\rangle$ is denoted by $\nu_n=n-\mu_1$.

On the basis of previously derived results [15] Eq. (15) can be interpreted as describing the Rydberg wave-packet dynamics in terms of propagation of the excited Rydberg electron in the photon-dressed channels $|\tilde{\Phi}_1(x)\rangle$ and $|\tilde{\Phi}_2(x)\rangle$. The Mth member of the sum in Eq. (15) can be assigned to a process in which the Rydberg electron performs M complete orbital round-trips around the nucleus after the initial excitation by the pump field. This excitation is characterized by the amplitudes $\tilde{\boldsymbol{\mathcal{D}}}_{g\mathbf{e}_a}^{(-)}(x)$. On each complete round-trip in the dressed channel j the Rydberg electron acquires a phase of magnitude $2\pi\tilde{\boldsymbol{\nu}}_{jj}(x)$ that is equal to the classical action of motion along a purely radial Kepler orbit with zero angular momentum and energy $\varepsilon-\tilde{\varepsilon}_{cj}(x)<0$. Between two round-trips the Rydberg electron may be scattered by the Rabi-oscillating ionic core. This process is described by the scattering matrix $\tilde{\boldsymbol{\chi}}(x)$. During the $(M+1)$th round-trip the atom leaves the standing-wave field and the state of the Rydberg electron is projected onto the bare Rydberg states $|n,1\rangle|\Phi_1\rangle$. This projection is described by the term in the first set of square brackets in Eq. (15). In Sec. III the influence of the internal electronic dynamics on the atomic center-of-mass motion will be discussed in detail with the help of the semiclassical path representation of Eq. (15).

In the above treatment, autoionization of the excited channel 2 and laser-induced transitions of the Rydberg electron to continuum states well above threshold have been neglected. However, the formalism may be adapted easily to the treatment of more general excitation processes in which these effects can be included [15]. Also, the spontaneous emission by the ionic core is not taken into account. This is justified as long as the interaction time between atom and standing wave is short in comparison to the spontaneous lifetime, which is of the order of several nanoseconds.

B. Experimental realization

In view of present-day experimental possibilities, the atomic diffraction experiment discussed above is somewhat idealized. Therefore, in the following an alternative, more realistic experimental setup is discussed briefly that involves short pulses.

Typical parameters in a realization of an experiment of the kind described above would be a mean excited quantum number around $\overline{\nu}=\nu(\overline{\varepsilon})=80$ corresponding to a classical orbit time of about $T_{\rm orb}=2\pi\overline{\nu}^3=80$ ps, an atomic center-of-mass velocity of $v_{\rm in}=1000$ ms^{-1}, a standing-wave laser field with a maximum intensity of the order of $I_{\rm max}=10$ kW cm^{-2}, and a wavelength λ between 250 and 450 nm. For these parameters the conditions for the applicability of the eikonal and Raman-Nath approximations are very well fulfilled. However, as the interaction times between atom and standing wave should be of the order of $T_{\rm orb}$, the standing wave would have to be focused onto a diameter of about 100 nm, which is smaller than the wavelength λ. A realiza-

tion of the standing wave with cw laser fields as described above would thus lead to severe practical difficulties and limitations.

An alternative that avoids these problems is the realization of the standing-wave field by two counterpropagating short pulses. A possible experiment could be performed in the following way. The standing wave is created by superposing two short optical pulses counterpropagating in the x direction. It is not necessary to focus them tightly; their diameter may be of the order of millimeters. In the spatial region where the two pulses overlap first, the standing wave exists for a time equal to the pulse duration. As soon as the standing wave has built up the short pump pulse is applied. In case the atom is inside the standing wave at the time the pump pulse is applied its interaction time with the standing wave therefore is not determined by its position in the z direction and its velocity. Instead, the interaction time depends only on the delay between the pump pulse and the destruction of the standing wave. This setup would thus allow one to carry out the experiment not only with single atoms but also with an atomic beam of higher intensity as it is no longer necessary to control the atomic z position. In order to guarantee a well-defined interaction time and field strength the profiles of the counterpropagating pulses should resemble the form of square pulses as closely as possible and their intensity should be spatially homogeneous. In addition, the diameter of the atomic beam should be small in comparison to the spatial extension of the optical pulse along the x direction.

This excitation scheme involving short laser pulses is a good approximation to the excitation process considered in Sec. II A. The entering and leaving of the standing-wave field by the atom is accomplished by creating and destroying the standing wave with the help of the counterpropagating short pulses. This scheme requires of course very good control of the shaping and synchronizing of the pulses involved, which does not seem to be out of reach in view of the rapid progress in the technology of manufacturing pulses [23,24]. Furthermore, as the relevant interaction time is determined only by the timing of the short laser pulses this experiment is not expected to be very sensitive to effects arising from the longitudinal velocity dispersion of the atomic beam. In order to increase the probability of excitation the short pump pulse $\mathcal{E}_a(t)$ should be of high intensity. If the pump pulse depletes the ground state on a time scale short in comparison to the wave-packet orbit time, the above derivation that originally assumed a weak pump pulse may easily be adapted to this case. One simply has to replace the pump pulse of Eqs. (4) and (5) by an exponential pulse, the decay time of which is twice the laser-induced depletion time of the initial state $|g\rangle$.

One could also think of performing the experiment by preparing the atoms in a Rydberg state $|n,1\rangle|\Phi_1\rangle$ before they enter the standing wave. In this case the short pump pulse would no longer be necessary. This setup would obscure the effects to be discussed in the next section significantly without, however, leading to their complete disappearance.

III. PHYSICAL DISCUSSION AND EXAMPLES

In this section the physical aspects of the question are discussed how the ICE-induced electron correlations influence the momentum transfer from a standing-wave light field to the atomic center of mass. For this purpose we consider the deflection of a fast atom by a standing-wave laser field as depicted in Fig. 1 schematically. Inside the standing-wave field an additional short laser pulse prepares an electronic Rydberg wave packet in the atom. In this way the standing wave is enabled to excite Rabi oscillations in the residual ionic core and to transfer transverse momentum to the atomic center of mass. This momentum transfer is influenced by the laser-induced interaction of the electronic Rydberg wave packet with the core electron. Its characteristics may be analyzed efficiently with the help of the theoretical tools derived in Sec. II A.

For the sake of clarity, the internal atomic dynamics will be described in terms of two non-autoionizing Rydberg series (Fig. 2). In Ref. [15] the neglect of autoionization was shown to be well justified for moderate autoionization rates and interaction times of the order of several wave-packet orbit times. However, autoionization could easily be taken into account in Eq. (15) with the help of complex quantum defects. In the absence of autoionization the laser-induced electron-electron correlation is determined solely by the extent of shakeup. A quantitative measure for this is given by the difference (mod 1) between the quantum defects of the two Rydberg series involved.

In the following numerical examples resonant excitation ($\Delta=\varepsilon_{c2}-\varepsilon_{c1}=0$) of a Rydberg wave packet with mean quantum number $\overline{\nu}=[2(\varepsilon_{c1}-\overline{\varepsilon})]^{-1/2}=80$ and $\mu_1=0.0$ is considered. The duration τ of the short pulse is equal to $0.3T_{\rm orb}$, with $T_{\rm orb}=2\pi\overline{\nu^3}=77.8$ ps unless otherwise stated. The envelope of the standing-wave laser field of Eq. (3) implies that the distribution of transverse momenta p_x of an atom leaving the interaction region with its core in the ground state contains only components equal to even multiples of the photon momentum k and that this momentum distribution is symmetric with respect to $p_x=0$. In the following examples only the part of the momentum distribution with $p_x\geqslant 0$ is shown. For the sake of clarity, it is depicted in the form of a continuous curve instead of discrete points at even multiples of k.

If the quantum defects of the resonantly coupled Rydberg series are equal, i.e., $\mu_1=\mu_2$, the dressed scattering matrix is given by $\tilde{\boldsymbol{\chi}}(x)=e^{2i\pi\mu_1}\mathbf{I}$ [15]. Thus the shakeup effect of the laser-induced core transitions on the wave-packet dynamics is minimal as no core scattering takes place between the photon-dressed core channels. The momentum transfer to the atomic center of mass, however, is determined by the characteristics of the Rydberg wave packet prepared. To discuss this momentum transfer it is convenient to sum up the geometric series in Eq. (15), which yields for the position-dependent probability amplitude

$$a_{n,1}^{(\mathcal{T})}(x)=(-1)^l e^{-i\overline{\varepsilon}t_0}\frac{d_{\varepsilon g}}{2\nu_n^{3/2}}[e^{-i\tilde{\varepsilon}_{n,+}(x)\mathcal{T}}\tilde{\mathcal{E}}_a(\tilde{\varepsilon}_{n,+}(x)-\overline{\varepsilon)}+e^{-i\tilde{\varepsilon}_{n,-}(x)\mathcal{T}}\tilde{\mathcal{E}}_a(\tilde{\varepsilon}_{n,-}(x)-\overline{\varepsilon)}]. \quad (18)$$

In this way the probability amplitude is expressed in terms of the contributions of the two dressed states $|n,\pm\rangle=(1/\sqrt{2})(|n,1\rangle\mp|n,2\rangle)$ in the standing-wave field pertaining to the two bare states $|n,1(2)\rangle$. Their energies are given by

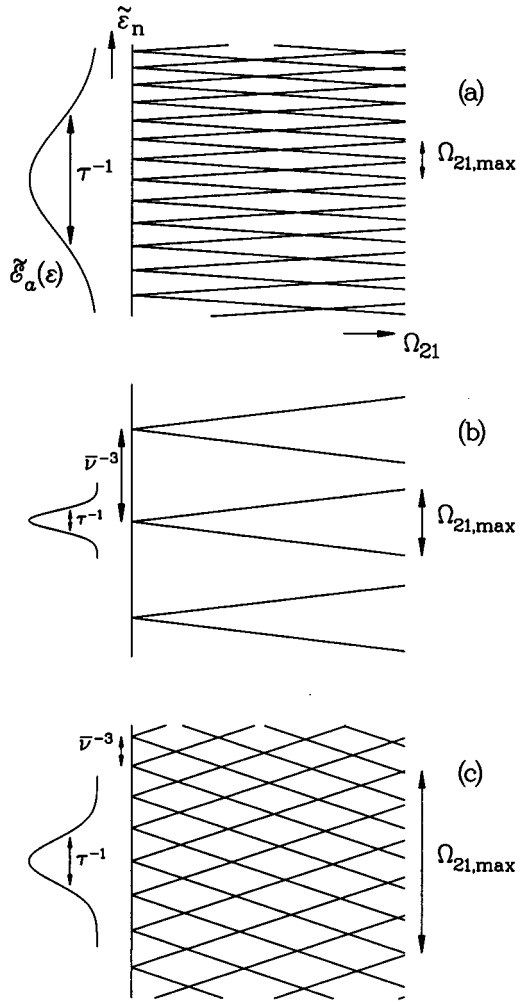

FIG. 3. The relation between the maximum induced Rabi frequency $\Omega_{21,\max}$, the excited energy range τ^{-1}, and the distance between adjacent bare Rydberg states $\overline{\nu^{-3}}=2\pi/T_{\rm orb}$ determines the characteristics of the momentum distribution in the case of equal quantum defects. This interplay is indicated by displaying the laser pulse shape $\tilde{\mathcal{E}}_a$ and the relevant excited dressed-state energies $\tilde{\varepsilon}_n$ as a function of Ω_{21} for the cases (a), (b), and (c) discussed in the text.

$\tilde{\varepsilon}_{n,\pm}(x)=\varepsilon_{c1}\pm\frac{1}{2}\Omega_{21}(x)$. According to Eq. (18), one can distinguish three limiting cases.

(a) $1/\tau\gg\Omega_{21,\max}$. The energy spread $1/\tau$ of the prepared wave packet is much larger than the maximum Rabi frequency $\Omega_{21,\max}$ or, in other words, the wave packet is prepared by the short pulse almost instantaneously in comparison with the characteristic time scale of the Rabi oscillations of the ionic core. In this case one may approximate $\tilde{\mathcal{E}}_a(\tilde{\varepsilon}_{n,+}(x)-\overline{\varepsilon})\approx\tilde{\mathcal{E}}_a(\tilde{\varepsilon}_{n,-}(x)-\overline{\varepsilon})\approx\tilde{\mathcal{E}}_a(\varepsilon_{n,1}-\overline{\varepsilon})$ [cf. Fig. 3(a)]. Therefore, in this case the deflection pattern is almost indistinguishable from the well-known one of a fast two-level atom that enters a standing-wave field (of rectangular shape) in its ground state and interacts with it for a time $\mathcal{T}$ [2]. As an example, in Fig. 4(a) the state-selective momentum distribution $P_{n,1}^{(\mathcal{T})}(p_x)=|a_{n,1}^{(\mathcal{T})}(p_x)|^2$ and the total distribution $P_1^{(\mathcal{T})}(p_x)=\Sigma_{n_1}P_{n,1}^{(\mathcal{T})}(p_x)$ summed over all Rydberg states are shown for $T_{\rm Rabi,min}=0.1T_{\rm orb}>\tau=0.03T_{\rm orb}$. They display the rapid oscillations familiar from the above-mentioned two-level case. The distributions $P_{n,1}^{(\mathcal{T})}(p_x)$ differ from each other only by a multiplicative constant that is due to the energy dependence of the envelope function $\tilde{\mathcal{E}}_a(\varepsilon)$.

(b) $1/\tau\ll\Omega_{21,\max}<2\pi/T_{\rm orb}$. This condition implies that, in general, only at most one pair of dressed states belonging to a certain principal quantum number n is excited [Fig. 3(b)]. As apparent from the condition $\tau\gg T_{\rm orb}$ the Rydberg electron is not prepared in the form of a wave packet. The momentum distribution could also be obtained from a pure two-level system that is excited correspondingly from a low-lying state. However, due to the strong position dependence of the excitation amplitudes $\tilde{\mathcal{E}}_a(\tilde{\varepsilon}_{n,+}(x)-\overline{\varepsilon})$ and $\tilde{\mathcal{E}}_a(\tilde{\varepsilon}_{n,-}(x)-\overline{\varepsilon})$ interesting effects may be observed. If one chooses, for example, $\overline{\varepsilon}$ equal to the energy of a bare Rydberg state, i.e., $\overline{\varepsilon}=\varepsilon_{n,1}$, then the atom is excited to the two dressed Rydberg states $|n,\pm\rangle$ only in the vicinity of the field nodes. There the induced light force (and thus the deflection) is large while the excitation in regions of weak induced light force is suppressed. In this way an efficient beam splitter is realized [Fig. 4(b)]. The maximum momentum transferred is approximately given by $|p_x|_{\max}=k\Omega_{21,\max}\mathcal{T}/2$.

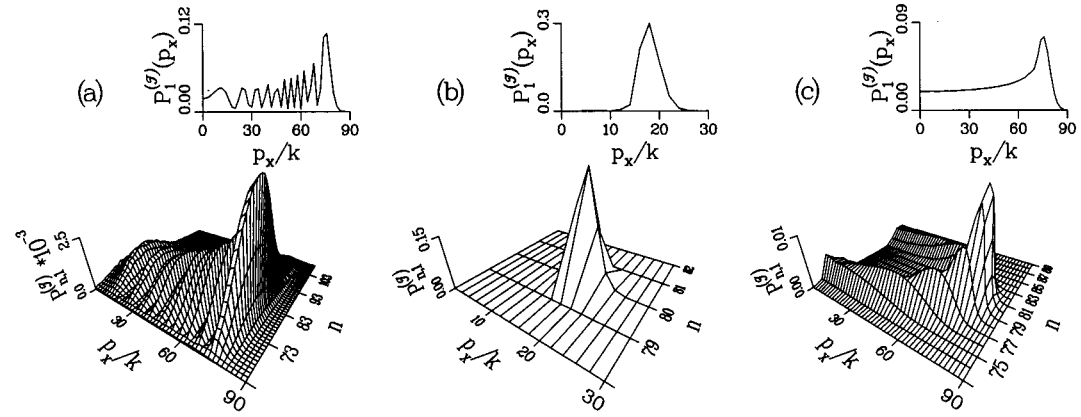

FIG. 4. State-selective momentum distributions $P_{n,1}^{(\mathcal{T})}=|a_{n,1}^{(\mathcal{T})}|^2$ and total momentum distributions $P_1^{(\mathcal{T})}=\Sigma_n P_{n,1}^{(\mathcal{T})}$ [both in units of $|(\mathcal{D}_{g\mathbf{e}_a}^{(-)})_1\mathcal{E}_a^{(0)}|^2\tau$] for $\mu_1=\mu_2=0.0$, $\overline{\nu}=80$, $\Delta=0$, and (a) $\mathcal{T}=2.5T_{\rm orb}$, $T_{\rm Rabi,min}=0.1T_{\rm orb}$, $\tau=0.03T_{\rm orb}$; (b) $\mathcal{T}=6.0T_{\rm orb}$, $T_{\rm Rabi,min}=1.0T_{\rm orb}$, $\tau=2.0T_{\rm orb}$; and (c) $\mathcal{T}=2.5T_{\rm orb}$, $T_{\rm Rabi,min}=0.1T_{\rm orb}$, $\tau=0.3T_{\rm orb}$.

(c) $1/\tau \ll \Omega_{21,\max}$ and $\Omega_{21,\max} > 2\pi/T_{\rm orb}$. Due to the second condition a number of dressed states with different principal quantum numbers n are excited significantly and, as expressed by the first condition, their excitation amplitudes vary strongly with position [Fig. 3(c)]. The resulting momentum distribution cannot be obtained with a two-level system and thus reflects the presence of the Rydberg wave packet. Figure 4(c) shows that the atomic deflection is indeed selective with respect to the Rydberg states. Dressed states of principal quantum number n with $|\varepsilon_{n,1} - \overline{\varepsilon}| < 1/\tau$ are excited only in the vicinity of the field nodes and are deflected strongly as described in case (b). States with $\Omega_{21,\max} > |\varepsilon_{n,1} - \overline{\varepsilon}| > 1/\tau$ are excited only in regions of weak stimulated light force and are therefore less deflected. In the latter case only one of the two dressed states $|n \pm\rangle$ is excited so that the momentum distribution does not display the usual oscillatory behavior. The state-selective deflection pattern in Fig. 4(c) can also be interpreted in an alternative way: It maps the position-dependent ac Stark splitting of the channel thresholds in the standing-wave onto the state-selective momentum distribution.

If the quantum defects of the resonantly coupled core channels are not equal, the Rabi oscillations of the ionic core cause a shakeup of the electronic Rydberg wave packet. Furthermore, Eq. (15) shows that any effects of shakeup can only be observed after the prepared electronic Rydberg wave packet has experienced at least one scattering from the laser-excited ionic core during the flight of the atom through the laser field.

In the extreme case of a maximal difference of the quantum defects, i.e., $\mu_2 - \mu_1 = 0.5$, these shakeup effects prevail. The corresponding scattering matrix that describes the laser-assisted core scattering between the photon-dressed core channels is given by

$$\tilde{\boldsymbol{\chi}}(x) = e^{2i\pi(\mu_1+\mu_2)} \begin{pmatrix} 0 & 1 \\ 1 & 0 \end{pmatrix}. \tag{19}$$

This scattering matrix is independent of the position x at which the atom crosses the standing-wave field because of the resonant character of the excitation. With each return to the core region the fractions of the initially prepared electronic Rydberg wave packet that propagate in the photon dressed core channels are scattered from one channel into the other one with a probability of unity. This extreme case of core scattering influences the momentum distribution of a diffracted atom significantly. In this context it is particularly interesting to study the width of the momentum distribution as a function of the interaction time between the standing-wave field and atom. This question is conveniently examined with the help of the semiclassical path expansion for the transverse momentum distribution given by Eqs. (14) and (15). The results of the analysis that is detailed in Ref. [25] and is based on a stationary-phase evaluation of the semiclassical path expansion may be summarized as follows.

(i) At interaction times equal to a small odd multiple of $T_{\rm orb}$, i.e., $\mathcal{T} = (2N+1)T_{\rm orb}$ with integer values of N up to about 5, to a good degree of approximation the maximum transferred momentum $|p_x|_{\max}$ is given by

$$|p_x|_{\max} = \frac{1}{2} k \Omega_{21,\max} T_{\rm orb}. \tag{20}$$

This value is independent of N. Like in the case of vanishing shakeup, the maximum momentum is transferred to atoms that cross the standing wave at the field nodes.

(ii) At interaction times equal to a small even multiple of $T_{\rm orb}$ the relation

$$|p_x|_{\max} = \frac{3}{8} k \Omega_{21,\max}^2 \mathcal{T} \left(\frac{T_{\rm orb}}{2\pi} \right)^{2/3} \tag{21}$$

holds. This result also applies to the case of large interaction times, irrespective of whether the number of returns is even or odd. The maximum transverse momentum of Eq. (21) grows linearly with $\mathcal{T}$. It is associated with atoms that cross the standing wave at positions with $\sin(2kx) = 0$ at which the electric-field strength does not vanish.

For interaction times $\mathcal{T}$ up to the order of several $T_{\rm orb}$ and maximum Rabi frequencies comparable to the mean excited level spacing $\overline{\nu_1^{-3}}$ Eqs. (20) and (21) imply that the maximum momentum transferred at odd multiples of $T_{\rm orb}$ is significantly larger than the one transferred at even multiples. The transverse momentum distribution is thus of oscillating width with respect to the interaction time. The laser-induced scattering process between the electronic Rydberg wave packet and the excited core electron causes the time evolution of the momentum transfer from the standing-wave laser field to the atom to be reversed at each return of the wave packet to the core. For larger interaction times the oscillations in the width of the distribution are gradually washed out. The core scatterings then manifest themselves in the fact that the maximum momentum transferred is much smaller than it would be in the absence of shakeup.

These characteristic features are exemplified in Fig. 5, where momentum distributions $P_1^{(\mathcal{T})}(p_x)$ are depicted for different values of interaction times with the standing-wave laser field. Figures 5(a)–5(d) illustrate the oscillation of the width of the momentum distribution as a function of the interaction time. They also confirm the more detailed predictions of Eqs. (20) and (21) as they show $|p_x|_{\max}$ to be approximately constant for odd multiples of $T_{\rm orb}$ while it increases proportionally to $\mathcal{T}$ at even multiples. The corresponding proportionality constant and the width of the distribution at odd multiples of $T_{\rm orb}$ are also in good quantitative agreement with the values inferred from Eqs. (20) and (21). However, for sufficiently large interaction times the maximum momentum transfer will be given by Eq. (21), approximately, irrespective of whether this interaction time corresponds to an even or odd number of returns of the excited Rydberg electron to the core. This behavior is apparent from Figs. 5(e) and 5(f).

For an intermediate difference in quantum defects, i.e., $0.0 < \mu_2 - \mu_1 < 0.5$, the dressed scattering matrix can be decomposed into a diagonal and an off-diagonal part, i.e., $\tilde{\boldsymbol{\chi}} = \tilde{\boldsymbol{\chi}}_{\rm diag} + \tilde{\boldsymbol{\chi}}_{\rm off}$. This decomposition reflects the fact that at each return to the nucleus the Rydberg wave packet may either be scattered between the dressed channels ($\tilde{\boldsymbol{\chi}}_{\rm off}$) or not ($\tilde{\boldsymbol{\chi}}_{\rm diag}$). As the foregoing discussion has shown, both processes have completely different effects on the momentum transfer from the standing-wave field to the atomic center of

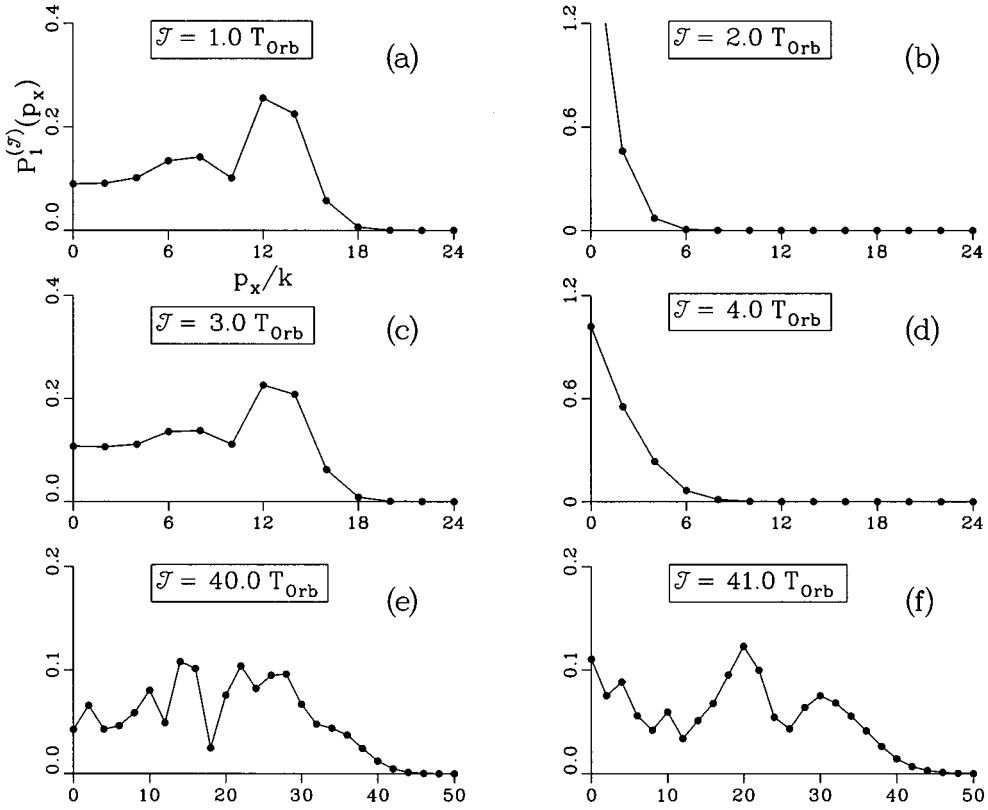

FIG. 5. Total momentum distribution $P_1^{(\mathcal{T})}(p_x)$ for parameters $\mu_1=0.0$, $\mu_2=0.5$, $T_{\mathrm{Rabi,min}}=0.2T_{\mathrm{orb}}$, and various interaction times $\mathcal{T}$ (other parameters as given in the text).

mass. As long as the core has not experienced a scattering of the wave packet between the dressed channels the momentum distribution grows linearly with time. However, as soon as such a scattering has taken place the momentum transfer is ''reversed'' and the momentum distribution begins to shrink. Correspondingly, subsequent scattering events lead to further ''reversals'' in the time development of the momentum transfer. As the events of scattering and nonscattering are superposed quantum mechanically, the momentum distribution consists of a superposition of the various distinct deflection patterns arising from the different ''scattering histories.'' Therefore, the internal dynamics of the atom that is determined by the interaction between the Rydberg wave packet and the ionic core is reflected in detail in the momentum distribution of the atomic center-of-mass motion.

The quantitative analysis of these kinds of processes may be accomplished easily with the help of Eqs. (14) and (15). As an example Fig. 6(a) shows the momentum distribution for an atom with $\mu_2-\mu_1=0.20$ and interaction time $\mathcal{T}=1.7T_{\mathrm{orb}}$. In this case only the $M=1$ term in Eq. (15) contributes significantly to the probability amplitude. The momentum distribution consists essentially of two distinct peaks around $p_x\approx 0$ and $p_x\approx 50k$. Using the decomposition of the dressed scattering matrix, the inner peak can be attributed to atoms in that the wave-packet fractions have experienced a scattering between the dressed channels at their first return to the nucleus, while the outer peak corresponds to atoms with unscattered wave-packet fractions [Fig. 6(b)]. Thus the internal dynamics is mapped onto the momentum distribution in a clear way. Figures 6(c) and 6(d) show the analysis of a more complicated deflection pattern at time $\mathcal{T}=2.5T_{\mathrm{orb}}$, where $M=2$ is dominant, in terms of the different histories connected with two wave-packet returns to the core. In this example, a time of approximately $0.5T_{\mathrm{orb}}$ has elapsed since the second return. The width of the contribution pertaining to atoms that have experienced no scatterings of the wave-packet fractions between the dressed channels (crosses) continues to grow linearly with $\mathcal{T}$. The distribution corresponding to a scattering at the second return (triangles), on the other hand, has begun to shrink due to the reversal effect. The distributions for scattering at the first return (circles and diamonds) are both rather narrow because the corresponding atoms did not possess any transverse momentum at the time of the second return of the wave packet. However, their width increases with growing interaction time.

The notion of the reversal effect may be defined more precisely. To this end we consider at a time $\mathcal{T}$ equal to an integer multiple q of T_{orb} a contribution to the momentum distribution that is characterized by a particular sequence of scattering and nonscattering events. For q not too large the width $|p_x|_{\max}$ of this contribution can be determined in the following way [25]. Between two returns to the core the width of the momentum distribution is changed by an amount of $\pm\Delta p$ with $\Delta p=\frac{1}{2}k\Omega_{21,\max}T_{\mathrm{orb}}$. The maximum momentum transferred to an atom is given by $|p_x|_{\max}=\Sigma_{i=1}^{q}\Delta p_i$. The contributions Δp_i are determined by the following rules: (a) $\Delta p_1=+\Delta p$; (b) if $\Sigma_{n=1}^{N}\Delta p_i=0$ for some $N<q$ then $\Delta p_{N+1}=+\Delta p$; (c) if $\Sigma_{n=1}^{N}\Delta p_i\neq 0$ then $\Delta p_{N+1}=\Delta p_N$ if the Rydberg wave packet is not scattered between

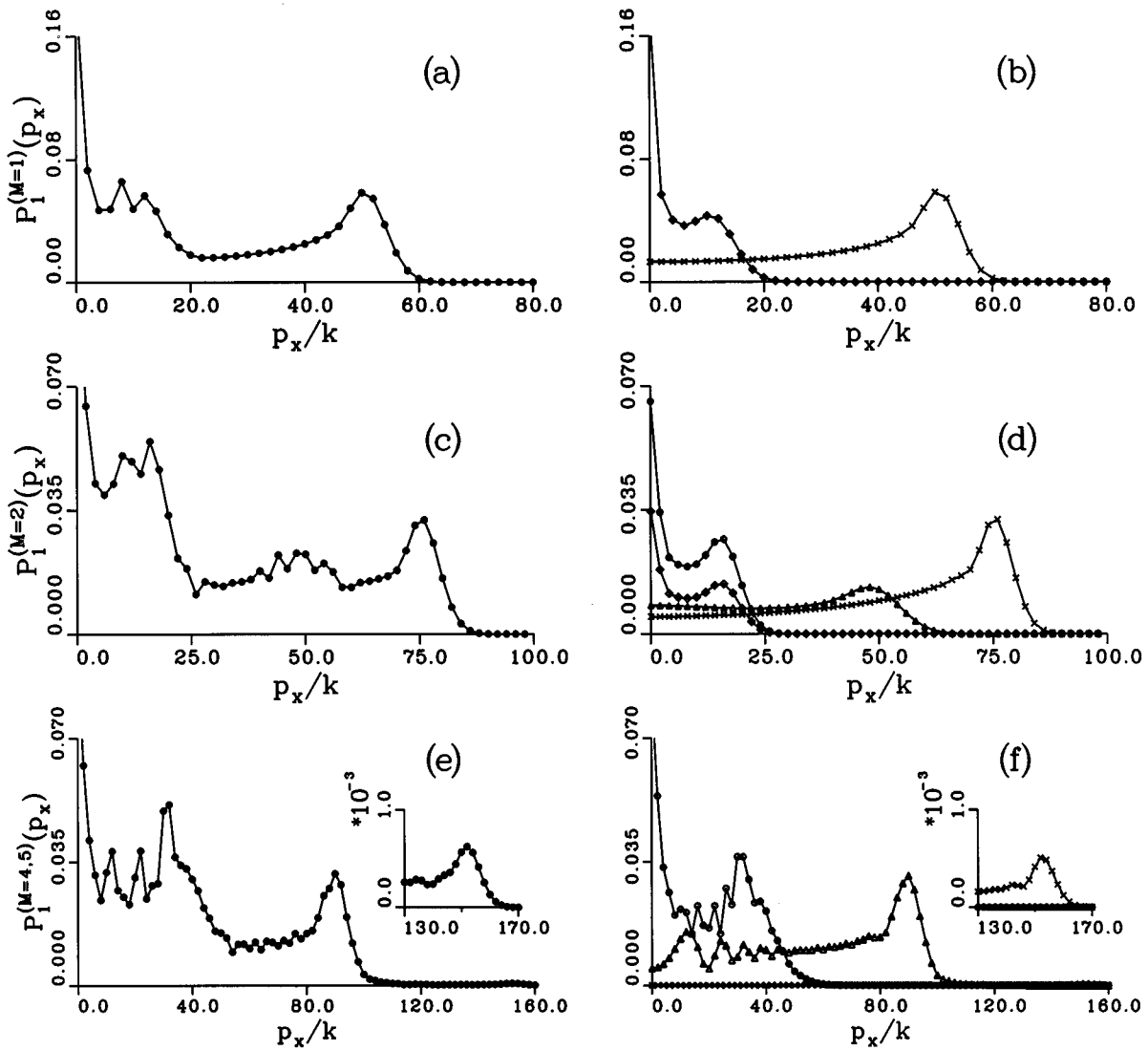

FIG. 6. (a) $M=1$ contribution $P_1^{(M=1)}$ [as evaluated from Eqs. (14) and (15)] to the total momentum distribution $P_1^{(T)}$ for parameters $\mu_1=0.0$, $\mu_2=0.2$, $T_{\mathrm{Rabi,min}}=0.1T_{\mathrm{orb}}$, and interaction time $\mathcal{T}=1.7T_{\mathrm{orb}}$ (other parameters as given in the text). (b) Contributions to $P_1^{(M=1)}$ from atoms in which the Rydberg wave packet has been scattered between the dressed channels at the first return to the core [$\diamond$, evaluated by replacing $\tilde{\chi}$ by $\tilde{\chi}_{\mathrm{off}}$ in Eq. (15)] and atoms in which the wave packet leaves the core unscattered ($\times$, evaluated with $\tilde{\chi}_{\mathrm{diag}}$). (c) Same as (a) but for $M=2$ and $\mathcal{T}=2.5T_{\mathrm{orb}}$. (d) Contributions to $P_1^{(M=2)}$ from atoms in which the wave packet has been scattered between the dressed channels twice ($\diamond$), only at the first return ($\bigcirc$), only at the second return ($\triangle$), and neither at the first nor the second return ($\times$). (e) Same as (a) but for $M=4,5$, $\mu_2=0.28$, and $\mathcal{T}=5.0T_{\mathrm{orb}}$. (f) Decomposition of $P_1^{(M=4,5)}$; for an explanation see the text.

the dressed channels at its Nth return to the core; otherwise $\Delta p_{N+1}=-\Delta p_N$.

As an example in Figs. 6(e) and 6(f) the transverse momentum distribution for parameters $\mu_2-\mu_1=0.28$, $T_{\mathrm{Rabi,min}}=0.1T_{\mathrm{orb}}$, and $\mathcal{T}=5T_{\mathrm{orb}}$ is analyzed. For this interaction time only the terms with $M=4,5$ contribute significantly to the transition amplitude (15). For the contribution of atoms in which the wave packet is not scattered at the first four returns to the core the above rules yield $|p_x|_{\max}=5\Delta p$, with $\Delta p=31.4k$. This contribution is shown in the magnification in Fig. 6(f) (crosses) and is evidently responsible for the outmost maximum in the total momentum distribution which occurs around $p_x\approx 152k$.

The contributions that are characterized by the sequences of scattering events ($snnn$), ($nnns$), ($ssnn$), ($nnss$), and ($nssn$) (with s denoting scattering and n nonscattering) all have a width of $3\Delta p$ according to the above rules. This is confirmed by the numerical calculation. The superposition of these contributions is depicted in Fig. 6(f) by the curve with triangles. It explains the behavior of the momentum distribution for $p_x>50k$. For all other contributions the above rules yield $|p_x|_{\max}=\Delta p$. This prediction is confirmed by the curve with circles in Fig. 6(f), which shows the superposition of these contributions and explains the momentum distribution for $p_x<50k$.

IV. SUMMARY AND CONCLUSIONS

The simultaneous laser excitation of two atomic valence electrons and their influence on the momentum transfer from a standing-wave laser field to the atomic center of mass have been investigated. This coherent momentum transfer that

originates from the stimulated light force leads to the deflection of atoms that traverse the standing-wave laser field. In particular, cases have been investigated in which during the flight of an atom through the standing-wave laser field one of these electrons is prepared as an electronic Rydberg wave packet by a short laser pulse and the other valence electron is excited resonantly to an energetically low-lying bound state by the standing-wave field.

A theoretical description of the resulting atomic deflection has been developed that is based on the dressed channel picture and semiclassical path representations of relevant transition amplitudes. In this approach the state-selective transition amplitudes of interest are represented as a sum of contributions originating from repeated returns of the laser-excited Rydberg electron to the ionic core during the interaction of the atom with the standing-wave laser field. With each return to the ionic core this Rydberg electron may be scattered from one photon-dressed core channel into the other. The probability amplitude describing the resulting momentum transfer to the atomic center of mass depends critically on the shakeup processes that are caused by these scatterings. Details of the internal electronic dynamics of an atom that crosses the standing-wave laser field manifest themselves in the momentum distribution of the deflected atom. Thus even different ''electronic scattering histories'' can be distinguished in this momentum distribution. This intricate interplay between laser-modified electron correlation effects and the atomic center-of-mass motion might have particularly interesting applications in atom optics.

ACKNOWLEDGMENT

This work was supported by the Deutsche Forschungsgemeinschaft within SFB 276.

APPENDIX: DERIVATION OF EQ. (15)

To derive the semiclassical path representation of Eq. (15) for the position-dependent probability amplitude $a_{n,1}^{(\mathcal{T})}(x)$ Eq. (12) is rewritten with the help of the resolvent of $H_0(x)$ and the closure relation for the radial Rydberg coordinate r in the form

$$a_{n,1}^{(\mathcal{T})}(x)=ie^{-i\overline{\varepsilon}t_0}\frac{-1}{2\pi i}\int_{-\infty+i0}^{\infty+i0}d\varepsilon\ e^{-i\varepsilon\mathcal{T}}\int_0^\infty dr\langle\Phi_1|\langle n,1|r\rangle \times\left\langle r\left|\frac{1}{\varepsilon-H_0(x)}\mathbf{d}\cdot\mathbf{e}_a\right|g\right\rangle\widetilde{\mathcal{E}}_a(\varepsilon-\overline{\varepsilon}). \quad \text{(A1)}$$

For the following, Coulomb functions of complex energy ε are defined by

$$C(r;\varepsilon)=\frac{i}{2}[\phi^{(-)}(r;\varepsilon)e^{2\pi i\nu(\varepsilon)}-\phi^{(+)}(r;\varepsilon)], \quad \text{(A2)}$$

with the effective quantum number $\nu(\varepsilon)=(-2\varepsilon)^{-1/2}$ and the energy normalized incoming- and outgoing Coulomb functions $\phi^{(\pm)}(r;\varepsilon)$ [18,20]. Except for ε real and positive the functions C converge to zero for $r\to\infty$. The radial wave functions appearing in Eq. (A1) can be evaluated for $r\geqslant r_c$ with the help of multichannel quantum-defect theory [20,26]. Thereby r_c denotes the radius of the ionic core, which is of the order of a few Bohr radii. Defining wave functions of bound states as in Ref. [20], one obtains

$$\langle n,1|r\rangle=(-1)^{l+1}\nu_n^{-3/2}e^{-i\pi\nu_n}C(r;\varepsilon_{n,1}-\varepsilon_{c1}) \quad (r\geqslant r_c), \quad \text{(A3)}$$

with $\varepsilon_{n,1}=\varepsilon_{c1}-1/[2(n-\mu_1^2)]$ denoting the energy of the Rydberg state $|n,1\rangle|\Phi_1\rangle$ and $\nu_n=\nu(\varepsilon_{n,1}-\varepsilon_{c1})$. Furthermore, the Green's function appearing in Eq. (A2) is given by [18]

$$\left\langle r\left|\frac{1}{\varepsilon-H_0(x)}\mathbf{d}\cdot\mathbf{e}_a\right|g\right\rangle=\widetilde{F}_1(r;\varepsilon,x)|\widetilde{\Phi}_1(x)\rangle+\widetilde{F}_2(r;\varepsilon,x)|\widetilde{\Phi}_2(x)\rangle, \quad \text{(A4)}$$

with

$$\widetilde{\mathbf{F}}(r;\varepsilon,x)=2\pi\widetilde{\mathbf{C}}(r;\varepsilon,x)[1-\widetilde{\boldsymbol{\chi}}(x)e^{2\pi i\widetilde{\boldsymbol{\nu}}(x)}]^{-1}\widetilde{\boldsymbol{\mathcal{D}}}_{g\mathbf{e}_a}^{(-)}(x) \quad (r\geqslant r_c) \quad \text{(A5)}$$

and $\widetilde{\mathbf{F}}^T=(\widetilde{F}_1,\widetilde{F}_2)$. All quantities appearing in Eqs. (A4) and (A5) have been defined in Sec. II except for the diagonal matrix $\widetilde{\mathbf{C}}_{jj}(r;\varepsilon,x)=C[r;\varepsilon-\widetilde{\varepsilon}_{cj}(x)]$. In order to perform the radial integration in Eq. (A1) one assumes that the main contributions come from values of r with $r\geqslant r_c$. In this way Eq. (15) is obtained by making use of the relation [21,27]

$$\int_{r_c}^\infty drC(r;\varepsilon_1)C(r;\varepsilon_2)=\frac{1}{2\pi i}\frac{e^{2\pi i\nu(\varepsilon_1)}-e^{2\pi i\nu(\varepsilon_2)}}{\varepsilon_1-\varepsilon_2} \quad \text{(A6)}$$

and expanding the inverted matrix of Eq. (A5) into a geometric series.

[1] P. E. Moskowitz, P. L. Gould, S. R. Atlas, and D. E. Pritchard, Phys. Rev. Lett. **51**, 370 (1983).

[2] A. P. Kazantsev, G. I. Surdutovich, and V. P. Yakovlev, *Mechanical Action of Light on Atoms* (World Scientific, Singapore, 1990).

[3] I. Sh. Averbukh, V. M. Akulin, and W. P. Schleich, Phys. Rev. Lett. **72**, 437 (1994).

[4] P. A. Ruprecht, M. J. Holland, and K. Burnett, Phys. Rev. A **49**, 4726 (1994).

[5] U. Janicke and M. Wilkens, Phys. Rev. A **50**, 3265 (1994).

[6] G. Alber, Phys. Rev. Lett. **69**, 3045 (1992); **70**, 2200 (1993).

[7] G. Alber and W. T. Strunz, Phys. Rev. A **50**, R3577 (1994).

[8] G. Alber, W. T. Strunz, and O. Zobay, Mod. Phys. Lett. B **8**, 1461 (1994).

[9] W. E. Cooke, T. F. Gallagher, S. A. Edelstein, and R. M. Hill, Phys. Rev. Lett. **40**, 178 (1978).

[10] T. F. Gallagher, *Rydberg Atoms* (Cambridge University Press, Cambridge, 1994).

[11] F. Robicheaux, Phys. Rev. A **47**, 1391 (1993).

[12] X. Wang and W. E. Cooke, Phys. Rev. A **46**, 4347 (1992).

[13] J. G. Story, D. I. Duncan, and T. F. Gallagher, Phys. Rev. Lett. **71**, 3431 (1993).
[14] L. G. Hanson and P. Lambropoulos, Phys. Rev. Lett. **74**, 5009 (1995).
[15] O. Zobay and G. Alber, Phys. Rev. A **52**, 541 (1995).
[16] N. J. van Druten and H. G. Muller, J. Phys. B **29**, 15 (1996).
[17] R. Scheunemann, Diploma thesis, Universität Freiburg im Breisgau, 1996 (unpublished).
[18] G. Alber and P. Zoller, Phys. Rep. **199**, 231 (1991).
[19] K. Gottfried, *Quantum Mechanics, Vol. I: Fundamentals* (Benjamin, Reading, MA, 1966).
[20] M. J. Seaton, Rep. Prog. Phys. **46**, 167 (1983).
[21] S. A. Bhatti, C. L. Cromer, and W. E. Cooke, Phys. Rev. A **24**, 161 (1981).
[22] G. Alber, H. Ritsch, and P. Zoller, Phys. Rev. A **34**, 1058 (1986).
[23] W. S. Warren, H. Rabitz, and M. Dahleh, Science **259**, 1581 (1993).
[24] Atomic deflection experiments involving standing waves created by short laser pulses are reported in, e.g., V. A. Grinchuk, E. F. Kuzin, M. L. Nagaeva, G. A. Ryabenko, A. P. Kazantsev, G. I. Surdutovich, and V. P. Yakovlev, Phys. Lett. **86A**, 136 (1981); V. A. Grinchuk, A. P. Kazantsev, E. F. Kuzin, M. L. Nagaeva, G. A. Ryabenko, G. I. Surdutovich, and V. P. Yakovlev, Zh. Éksp. Teor. Fiz. **86**, 100 (1984); J. Opt. Soc. Am. B **2**, 1805 (1985).
[25] O. Zobay, Ph.D. dissertation, Universität Freiburg im Breisgau, 1996 (unpublished).
[26] U. Fano and A. R. P. Rau, *Atomic Collisions and Spectra* (Academic, New York, 1986).
[27] R. H. Bell and M. J. Seaton, J. Phys. B **18**, 1589 (1985).